Cambrian cinctan echinoderms shed light on feeding in the ancestral deuterostome

Imran A. Rahman[1*], Samuel Zamora[2], Peter L. Falkingham[3] and Jeremy C. Phillips[1]

[1]School of Earth Sciences, University of Bristol, Wills Memorial Building, Queen's Road, Bristol BS8 1RJ, UK

[2]Instituto Geológico y Minero de España, C/ Manuel Lasala, 44 - 9º B, 50006 Zaragoza, Spain

[3]School of Natural Sciences and Psychology, Liverpool John Moores University, Byrom Street, Liverpool L3 3AF, UK

***Author for correspondence:**

Imran A. Rahman

e-mail: imran.rahman@bristol.ac.uk

Abstract

Reconstructing the feeding mode of the latest common ancestor of deuterostomes is key to elucidating the early evolution of feeding in chordates and allied phyla; however, it is debated whether the ancestral deuterostome was a tentaculate feeder or a pharyngeal filter feeder. To address this, we evaluated the hydrodynamics of feeding in a group of fossil stem-group echinoderms (cinctans) using computational fluid dynamics. We simulated water flow past three-dimensional digital models of a Cambrian fossil cinctan in a range of possible life positions, adopting both passive tentacular feeding and active pharyngeal filter feeding. The results demonstrate that an orientation with the mouth facing downstream of the current was optimal for drag and lift reduction. Moreover, they show that there was almost no flow to the mouth and associated marginal groove under simulations of passive feeding, whereas considerable flow towards the animal was observed for active feeding, which would have enhanced the transport of suspended particles to the mouth. This strongly suggests that cinctans were active pharyngeal filter feeders, like modern enteropneust hemichordates and urochordates, indicating that the ancestral deuterostome employed a similar feeding strategy.

Keywords:

echinoderms, deuterostomes, evolution, feeding, functional morphology, computational fluid dynamics

1. Introduction

Deuterostomes are one of the three major clades of bilaterian animals. Molecular phylogenetics has helped resolve the relationships of the main deuterostome phyla (chordates, echinoderms and hemichordates) [1–3], but despite extensive study of their anatomy, development and phylogeny for over a century, important aspects of the early evolutionary history of deuterostomes remain unclear [4]. Feeding is one such outstanding issue; it was long speculated that the ancestral deuterostome had tentacles for collecting food from the water column, like modern crinoids and pterobranch hemichordates [5–7], but more recently it has been proposed that it had a pharynx with gill slits for actively generating feeding currents, similar to enteropneust hemichordates, urochordates, cephalochordates and larval lampreys [8–10]. Distinguishing between these competing hypotheses is problematic because it is disputed whether the latest common ancestor of deuterostomes had a pterobranch-like body plan (with tentacular feeding), or an enteropneust-like body plan (with pharyngeal filter feeding) [4].

The fossil record provides an alternative means of differentiating these two hypotheses through the inference of feeding modes in the earliest fossil forms, and could thus inform on the ancestral feeding strategy of deuterostomes. Although the early record of most deuterostome phyla is patchy and incomplete [4], echinoderms possess a rich record dating back to the Cambrian [11,12] because a mineralized skeleton was among their first derived traits [13]. Several groups of pre-radiate fossil stem-group echinoderms (*Ctenoimbricata*, ctenocystoids and cinctans) are especially important, as they document the earliest steps in the assembly of the echinoderm body plan and retain plesiomorphic characters of the ancestral deuterostome [14–16]. Cinctans are the best understood of these groups in terms of their anatomy and functional morphology, and so have the greatest potential for elucidating deuterostome evolution; however, their mode of feeding is controversial. It is widely

accepted that cinctans were sessile epibenthic suspension feeders with an anterolateral mouth and one or a pair of marginal grooves [7,14,17–20], but it is debated whether they were passive suspension feeders with a system of tentacles, analogous to crinoids [19,20], or active pharyngeal filter feeders, similar to urochordates [14,21].

In order to evaluate competing hypotheses of cinctan feeding mode, we quantitatively analysed the functional performance of a Cambrian fossil cinctan. Using three-dimensional computational fluid dynamics (CFD), we simulated flow past a digital reconstruction of the fossil in a range of different positions relative to the current direction and the sediment–water interface, approximating both hypothesized feeding scenarios. The results provide new insights into the hydrodynamics of feeding in cinctans, with implications for the plesiomorphic mode of feeding in deuterostomes.

2. Material and methods

(a) Fossil specimen

The holotype of the cinctan *Protocinctus mansillaensis* (MPZ 2004/170; Museo Paleontológico de la Universidad de Zaragoza, Spain) was selected for use in CFD simulations owing to its exceptional three-dimensional preservation as recrystallized calcite. This species comes from the Mansilla Formation of Purujosa, north-east Spain, which is early middle Cambrian (Cambrian Series 3, Stage 5) in age (~510 Ma) and is characterized by purple to reddish nodular limestones and shales, indicative of a shoreface to offshore depositional setting. Like all cinctans, *Protocinctus* has a flattened, asymmetrical body

(theca) and a rigid posterior appendage. A circular mouth is located on the anterior right side of the theca; a larger exhalant aperture (the porta) is situated at the anterior midline of the theca, covered by a movable plate (the operculum). *Protocinctus* is also characterized by an elongate, oval-shaped theca, a single left marginal groove and a weakly-developed ventral swelling at the anterior (figure 1*a*).

(b) X-ray micro-tomography

The fossil was scanned with a Phoenix v|tome|x s system and digitally reconstructed using the SPIERS software suite [22]. See Rahman and Zamora [23] for details. A ZIP archive containing the digital reconstruction in VAXML format can be downloaded from Dryad (doi:10.5061/dryad.g4n5m).

(c) Digital restoration

In order to restore the poorly-preserved upper surface of the studied specimen, the dorsal integument and the operculum were virtually extrapolated in SPIERS with a closed spline (using other specimens in which the upper surface is better preserved as a reference). The operculum was restored in two hypothetical life positions: (1) 'closed', with the porta entirely covered by the operculum (figure 1*b*) and (2) 'open', with the operculum raised above the porta (figure 1*c*). These reconstructions were then optimized with a low smoothing value to remove noise, and converted into NURBS surfaces using Geomagic Studio (www.geomagic.com) (models can be downloaded from Dryad: doi:10.5061/dryad.g4n5m).

(d) Computational fluid dynamics simulations

CFD simulations of water flow around *Protocinctus* were performed using COMSOL Multiphysics (www.uk.comsol.com). The computational domain consisted of a three-

dimensional volume above a flat solid boundary (85 mm in length and 17.5 mm in diameter), on which the *Protocinctus* reconstruction (23 mm in length and 10 mm in width) was centrally fixed (electronic supplementary material, figure S1*a*). Flow was simulated through this domain with an initially uniform inflow velocity at the upstream end and an outflow boundary condition (zero pressure gradient across the boundary) at the downstream end. Slip conditions (zero stress across the boundary) were used for the domain sides and top, with no-slip conditions (zero velocity relative to the boundary) for the solid surfaces of the reconstruction and the underlying base. The flow domain was a semi-cylinder and was sufficiently large that the boundary conditions did not influence the flow. The domain was meshed using free tetrahedral elements (electronic supplementary material, figure S1*b*), with mesh resolution fully tested to ensure grid scale independence for the simulation results (electronic supplementary material, sensitivity analyses).

A total of 100 simulations were undertaken, using a range of input parameters (electronic supplementary material, table S1). In all cases, three-dimensional, incompressible (constant density) flow of water was simulated, with the *Protocinctus* reconstruction held stationary. Ambient flow velocities of 0.05, 0.1 or 0.2 m/s (Reynolds numbers of 525–925, 1050–1850 and 2100–3700, respectively; width of the specimen in the flow taken as the characteristic dimension) were simulated to approximate typical near-bottom currents in modern shoreface to offshore environments [24]. A stationary solver was used to compute the steady-state flow patterns and a laminar flow model was used to solve the Navier-Stokes equations for conservation of momentum and the continuity equation for conservation of mass. The effects of varying the solver type and flow model were examined for the higher Reynolds number flows (electronic supplementary material, sensitivity analyses). In addition, experimental studies of flow around a 3-D printed model of *Protocinctus* were carried out in a flume tank

for comparison with the computer simulations (electronic supplementary material, flume tank experiments, figure S2).

Three different feeding scenarios were simulated. (1) Passive tentacular feeding using the closed *Protocinctus* reconstruction with the mouth cross-section allowing flow to pass through (outflow boundary). (2) The inhalant current of active pharyngeal filter feeding using the closed *Protocinctus* reconstruction with flow velocity through the mouth cross-section given a normal outflow velocity of 0.015 m/s. (3) The exhalant current of active pharyngeal filter feeding using the open *Protocinctus* reconstruction with flow velocity through the operculum cross-section given a normal inflow velocity of 0.04 m/s. The inhalant and exhalant velocities of pharyngeal filter feeding were based on analogy with the extant urochordate *Styela clava* [25].

To explore the hydrodynamic consequences of different life positions, all of the above simulations were performed with the *Protocinctus* reconstruction oriented at 0°, 45°, 90°, 135° and 180° to the current, and with the ventral swelling positioned either below (equivalent to burial within the sediment) or on top of (equivalent to resting on the sediment) the lower boundary of the computational domain. The results were visualized as two-dimensional cross-sections of flow velocity magnitude with flow vectors (arrows) and streamlines. Drag and lift forces and their coefficients (projected frontal area taken as the reference area) were calculated to quantify flow around the digital reconstructions.

3. Results

The results of the CFD simulations show that the overall characteristics of the flow around the *Protocinctus* reconstruction conformed to expectations for boundary layer and wake development. In all cases, the velocity decreased rapidly immediately upstream of the *Protocinctus* reconstruction (figure 2; electronic supplementary material, figures S3–S8) and a distinctive wake (elongate, low-velocity flow region, typically with an asymmetrical vortex) was formed immediately downstream. The size and shape of the wake varied depending on the orientation of the reconstruction to the current, but were not significantly affected by the simulated feeding scenario, or the placement of the reconstruction in relation to the lower boundary of the domain (figure 2; electronic supplementary material, figures S3–S8). A characteristic boundary layer, shown by a rapid drop in velocity as the flow approached the bottom of the domain, was well developed in all the simulations. The thickness of the boundary layer was roughly equal to the height of the *Protocinctus* reconstruction in both positions relative to the underlying base (figure 2).

Distinctly different flow patterns were associated with different feeding scenarios. Flow vectors and streamlines indicate that the velocity of the flow into the mouth was greatest in the simulations of the inhalant current generated by pharyngeal filter feeding (figure 2*g–l*; electronic supplementary material, figures S5 and S6). This was most pronounced when the *Protocinctus* reconstruction was oriented at 180° to the current. Conversely, in the simulations where there was no inhalant current, flow into the mouth was generally much weaker (figure 2*a–f*, *m–r*; electronic supplementary material, figures S3, S4, S7 and S8). Flow to the marginal groove was very low for all the simulated feeding modes (electronic supplementary material, figure S9).

In the simulations of the exhalant current produced by pharyngeal filter feeding, a jet of high-velocity flow passed out of the porta, intruding into the ambient flow or the wake, depending on the orientation of the reconstruction (figure 2*m–r*; electronic supplementary material, figures S7 and S8). When the *Protocinctus* reconstruction was oriented at 0° to the current, this jet directly opposed the ambient flow direction (electronic supplementary material, figures S7*a–c* and S8*a–c*), whereas with the reconstruction oriented at 180° to the current, it flowed in the same direction as the ambient flow, contributing to the wake (figure 2*m–r*).

Consistent with theoretical expectations, the drag force exerted by the reconstruction on the fluid flow increased as the ambient velocity increased, whereas the drag coefficient decreased. The lift force also increased with increasing ambient velocity. The orientation of the reconstruction strongly influenced both the drag and lift forces and the lift coefficient, which were greatest when the reconstructions were oriented at 45°, 90° or 135° to the current. The reconstruction position relative to the domain bottom was likewise important, with the drag and lift forces and the drag coefficient higher when the ventral swelling was positioned on top of the lower boundary of the domain (figure 3; electronic supplementary material, figures S10 and S11, tables S2 and S3).

The results of the simulations were not greatly influenced by varying the mesh size, solver or flow type, with all these analyses producing very similar flow structures, drag and lift (electronic supplementary material, figures S12–S14, table S4). Moreover, comparisons between the experimental studies and the computer simulations showed that both approaches obtained similar downstream current velocities (electronic supplementary material, figure S15).

4. Discussion

CFD simulations indicate that orientation had a marked effect on the amount of drag generated by *Protocinctus*, with the largest wake size and highest drag force occurring when the reconstruction was oriented at 45°, 90° or 135° to the current (figure 3; electronic supplementary material, figures S3–S8, table S2). The lift force and coefficient were also greatest when the reconstruction was non-parallel to the current (figure 3; electronic supplementary material, figure S11, table S3). Drag and lift can be detrimental to epibenthic organisms, making it harder to maintain posture and even dislodging or injuring animals [26,27]. While some suspension feeders seek to increase drag to aid feeding [26], this was almost certainly not the case for *Protocinctus*, which exhibits a streamlined profile (figure 1) that is clearly adapted to reduce drag parallel to the flow direction. Therefore, it seems most probable (on functional grounds) that *Protocinctus* was preferentially oriented parallel to the current in life, minimizing both drag and lift. Simulations with the reconstruction facing upstream and downstream produced similar amounts of drag (figure 3; electronic supplementary material, figure S10, table S2). However, the lift was substantially greater when the reconstruction faced upstream (figure 3; electronic supplementary material, figure S11, table S3). Moreover, the simulations of the exhalant current clearly show that the jet of exhalant flow out of the porta would have been transported to the mouth by the ambient flow if the reconstruction faced into the current (electronic supplementary material, figures S7*a–c* and S8*a–c*). Because the porta is interpreted as an exhalant opening under both passive [19,20] and active [14,21] feeding scenarios, an upstream orientation would have led to fouling of the mouth and associated marginal groove in either mode of feeding. Consequently, it can be inferred that cinctans were oriented downstream in life, and this

agrees with previous interpretations of cinctan functional morphology [7,19,21] and a qualitative flume study [18], which suggested that an orientation with the mouth facing away from the prevailing current would have enhanced feeding and/or stability.

The flow structure did not vary appreciably according to the position of *Protocinctus* relative to the sediment–water interface, but the drag and lift forces were higher in the simulations of the ventral swelling resting on top of the sediment surface (figure 3; electronic supplementary material, tables S2 and S3). This suggests that a position with the ventral swelling buried was optimal for reducing drag and lift, and might also have been beneficial for anchoring the animal to the seafloor [17,28]. Regardless of the placement of the ventral swelling, however, *Protocinctus* would always have been situated in the low-velocity boundary layer, with the mouth and marginal groove close to the sediment surface (figure 2). This position has implications for the interpretation of the animal's mode of feeding. The simulations of passive feeding with *Protocinctus* in a downstream orientation demonstrate that there was almost no flow to the mouth and adjacent marginal groove (figure 2*a–f*; electronic supplementary material, figure S9), indicating that the transport of suspended particles to the animal would have been extremely limited. Nutrient flux is known to be very low within the boundary layer [29], and modern passive suspension feeders typically possess specialized food-capturing structures, such as fans, nets or tentacles, which are elevated above this zone, where there are higher rates of flow and nutrient flux, to facilitate feeding [26,30]. There is no evidence of such morphological adaptations in cinctans, which are characterized by a flattened body with recumbent feeding structures (mouth and marginal groove). Thus, if cinctans faced downstream (as argued above) and relied on external flows alone, they would have had access to a very limited supply of nutrients, which was likely insufficient for passive tentaculate feeding.

CFD simulations provide better support for an active pharyngeal filter feeding mode of life. The inhalant current generated by *Protocinctus* channelled considerable flow towards the animal (figure 2*g–l*), which would have enhanced the transport of suspended particles into the mouth. Furthermore, simulations of active feeding with *Protocinctus* facing downstream show that the exhalant jet ejected from the porta travelled above any recirculating flow in the wake close to the mouth and marginal groove, avoiding potential contamination of feeding currents (figure 2*m–r*). The same pattern is documented in extant pharyngeal filter feeders, such as urochordates, which are capable of generating powerful exhalant flows that carry wastewater beyond the mouth [25,26]. Consequently, simulations of both inhalant (figure 2*g–l*) and exhalant (figure 2*m–r*) currents are compatible with pharyngeal filter feeding, and this agrees with studies of cinctans that suggested such a feeding mode based on the functional morphology of the porta–operculum complex and detailed comparisons with urochordates [14,18,21].

Our findings are broadly in agreement with previous interpretations of the earliest fossil stem-group echinoderms (*Ctenoimbricata*, ctenocystoids and cinctans) as pharyngeal filter feeders [14–16], and argue against their interpretation as passive tentaculate feeders [19,20]. Among modern deuterostomes, active suspension feeding with pharyngeal gill slits is documented in enteropneust hemichordates, urochordates, cephalochordates and larval lampreys, while suspension feeding with tentacles characterizes crinoids and pterobranch hemichordates. Owing to their position close to the base of echinoderm phylogeny, the inference of pharyngeal filter feeding in cinctans allows us to extend this feeding mode back to the latest common ancestor of all deuterostomes (figure 4). This provides strong support for the hypothesis that the ancestral deuterostome fed through pharyngeal filtering [8–10],

indicating that a pharynx with gill slits is in all likelihood a deuterostome symplesiomorphy and that the tentacular feeding systems of echinoderms and pterobranchs are most probably not homologous.

Data accessibility. Digital models of *Protocinctus* and a video file can be downloaded from Dryad (doi:10.5061/dryad.g4n5m).

Competing interests. We have no competing interests.

Authors' contributions. IAR and PLF conceived the study. IAR and JCP carried out CFD simulations. IAR wrote the paper and prepared figures/tables. All authors analysed the data, reviewed drafts of the paper and gave final approval for publication.

Acknowledgements. We thank Benedict Rogers (University of Manchester) for advice on modelling, Keith Adcock (Birmingham City University) for 3-D printing and Gareth Keevil (University of Leeds) for assistance with flume tank experiments. Phil Donoghue and Stephan Lautenschlager (University of Bristol) provided helpful comments on an earlier version of the text, and the final version benefited greatly from the comments of three anonymous referees.

Funding. Imran Rahman was supported by an 1851 Royal Commission Research Fellowship. Samuel Zamora acknowledges a Ramón y Cajal Grant (RYC-2012-10576) and project CGL2013-48877 from the Spanish Ministry of Economy and Competitiveness.

315

316 ## References

317

318 1. Bourlat SJ, Juliusdottir T, Lowe CJ, Freeman R, Aronowicz J, Kirschner M, Lander ES,
319 Thorndyke M, Nakano H, Kohn AB, *et al.* 2006 Deuterostome phylogeny reveals
320 monophyletic chordates and the new phylum Xenoturbellida. *Nature* **444**, 85–88.
321 (doi:10.1038/nature05241)
322 2. Philippe H, Brinkmann H, Copley RR, Moroz LL, Nakano H, Poustka AJ, Wallberg A,
323 Peterson KJ, Telford MJ. 2011 Acoelomorph flatworms are deuterostomes related to
324 *Xenoturbella*. *Nature* **470**, 255–258. (doi:10.1038/nature09676)
325 3. Cannon JT, Kocot KM, Waits DS, Weese DA, Swalla BJ, Santos SR, Halanych KM.
326 2014 Phylogenomic resolution of the hemichordate and echinoderm clade. *Curr. Biol.* **24**,
327 2827–2832. (doi:10.1016/j.cub.2014.10.016)
328 4. Swalla BJ, Smith AB. 2008 Deciphering deuterostome phylogeny: molecular,
329 morphological and palaeontological perspectives. *Phil. Trans. R. Soc. B* **363**, 1557–1568.
330 (doi:10.1098/rstb.2007.2246)
331 5. Romer AS. 1967 Major steps in vertebrate evolution. *Science* **158**, 1629–1637.
332 (doi:10.1126/science.158.3809.1629)
333 6. Gee H. 1996 *Before the backbone: views on the origin of vertebrates*. London: Chapman
334 and Hall.
335 7. Jefferies RPS, Brown NA, Daley PEJ. 1996 The early phylogeny of chordates and
336 echinoderms and the origin of chordate left–right asymmetry and bilateral symmetry.
337 *Acta Zool., Stockholm* **77**, 101–122. (doi:10.1111/j.1463-6395.1996.tb01256.x)

8. Cameron CB. 2002 Particle retention and flow in the pharynx of the enteropneust worm *Harrimania planktophilus*: the filter-feeding pharynx may have evolved before the chordates. *Biol. Bull.* **202**, 192–200.
9. Cameron CB. 2005 A phylogeny of the hemichordates based on morphological characters. *Can. J. Zool.* **83**, 196–215. (doi:10.1139/Z04-190)
10. Gonzalez P, Cameron CB. 2009 The gill slits and pre-oral ciliary organ of *Protoglossus* (Hemichordata: Enteropneusta) are filter-feeding structures. *Biol. J. Linn. Soc.* **98**, 898–906. (doi:10.1111/j.1095-8312.2009.01332.x)
11. Zamora S, Lefebvre B, Álvaro JJ, Clausen S, Elicki O, Fatka O, Jell P, Kouchinski A, Lin J-P, Nardin E, Parsley R, Rozhnov S, Sprinkle J, Sumrall CD, Vizcaïno D, Smith AB. 2013 Global Cambrian echinoderm diversity and palaeobiogeography. In *Early Palaeozoic biogeography and palaeogeography* (eds Harper DAT, Servais T), pp. 151–164. *Geological Society, London, Memoirs* **38**, 490 pp.
12. Zamora S, Rahman IA. 2014 Deciphering the early evolution of echinoderms with Cambrian fossils. *Palaeontology* **57**, 1105–1119. (doi:10.1111/pala.12138)
13. Bottjer DJ, Davidson EH, Peterson KJ, Cameron RA. 2006 Paleogenomics of echinoderms. *Science* **314**, 956–960. (doi:10.1126/science.1132310)
14. Smith AB. 2005 The pre-radial history of echinoderms. *Geol. J.* **40**, 255–280. (doi:10.1002/gj.1018)
15. Rahman IA, Clausen S. 2009 Re-evaluating the palaeobiology and affinities of the Ctenocystoidea (Echinodermata). *J. Syst. Palaeontol.* **7**, 413–426. (doi:10.1017/S1477201909990046)
16. Zamora S, Rahman IA, Smith AB. 2012 Plated Cambrian bilaterians reveal the earliest stages of echinoderm evolution. *PLoS ONE* **7**, e38296. (doi:10.1371/journal.pone.0038296)

17. Ubaghs G. 1968 Homostelea. In *Treatise on invertebrate paleontology, part S, Echinodermata 1 (2)* (ed. Moore RC), pp. S565–S581. Boulder and Lawrence: Geological Society of America and University of Kansas Press.
18. Friedrich W-P. 1993 Systematik und Funktionsmorphologie mittelkambrischer Cincta (Carpoidea, Echinodermata). *Beringeria* **7**, 3–190.
19. Parsley RL. 1999 The Cincta (Homostelea) as blastozoans. In *Echinoderm research 1998* (eds Candia Carnevali MD, Bonasoro F), pp. 369–375. Rotterdam: Balkema.
20. David B, Lefebvre B, Mooi R, Parsley R. 2000 Are homalozoans echinoderms? An answer from the extraxial-axial theory. *Paleobiology* **26**, 529–555. (doi:10.1666/0094-8373(2000)026<0529:AHEAAF>2.0.CO;2)
21. Zamora S, Smith AB. 2008 A new Middle Cambrian stem-group echinoderm from Spain: palaeobiological implications of a highly asymmetric cinctan. *Acta Palaeontol. Pol.* **53**, 207–220. (doi:10.4202/app.2008.0204)
22. Sutton MD, Garwood RJ, Siveter DJ, Siveter DJ. 2012 SPIERS and VAXML; a software toolkit for tomographic visualisation and a format for virtual specimen interchange. *Paleontol. Electron.* **15/5T**, 14 pp. (http://palaeo-electronica.org/content/issue-2-2012-technical-articles/226-virtual-palaeontology-toolkit)
23. Rahman IA, Zamora S. 2009 The oldest cinctan carpoid (stem-group Echinodermata), and the evolution of the water vascular system. *Zool. J. Linn. Soc.* **157**, 420–432. (doi:10.1111/j.1096-3642.2008.00517.x)
24. Emelyanov EM. 2005 *The barrier zones in the ocean*. New York: Springer.
25. Riisgård HU. 1988 The ascidian pump: properties and energy cost. *Mar. Ecol. Prog. Ser.* **47**, 129–134. (doi:10.3354/meps047129)
26. Vogel S. 1996 *Life in moving fluids*. Princeton: Princeton University Press.

27. Koehl MAR. 1984 How do benthic organisms withstand moving water? *Am. Zool.* **24**, 57–70. (doi:10.1093/icb/24.1.57)

28. Ubaghs G. 1975. Early Paleozoic echinoderms. *Annu. Rev. Earth Pl. Sc.* **3**, 79–98. (doi:10.1146/annurev.ea.03.050175.000455)

29. Jumars PA, Gallagher ED. 1982 Deep-sea community structure: three plays on the benthic proscenium. In *The environment of the deep sea* (eds Ernst WG, Morin JG), pp. 217–285. Englewood Cliffs: Prentice Hall.

30. LaBarbera M. 1984 Feeding currents and particle capture mechanisms in suspension feeding animals. *Am. Zool.* **24**, 71–84. (doi:10.1093/icb/24.1.71)

Figure captions

Figure 1. *Protocinctus mansillaensis*. (*a*) Original fossil specimen (ventral view). (*b*) Digital restoration with the operculum closed (anterolateral view). (*c*) Digital restoration with the operculum open (anterolateral view). (*d*) Digital restoration with the operculum closed (lateral view).

Figure 2. Results of the CFD simulations with *Protocinctus* oriented at 180° to the current, visualized as two-dimensional plots (horizontal and vertical cross-sections) of flow velocity magnitude (false-colour scale different for each ambient flow velocity) with flow vectors (arrows; length of arrows proportional to the natural logarithm of the flow velocity magnitude) and streamlines. (*a–f*) Simulations of passive tentacular feeding. (*g–l*) Simulations of the inhalant current of pharyngeal filter feeding. (*m–r*) Simulations of the

411 exhalant current of pharyngeal filter feeding. The mouth is indicated by a *, the porta is
412 indicated by a +. The ambient flow is from left to right.
413
414 **Figure 3.** Drag and lift forces for the CFD simulations. (*a*–*c*) Simulations of passive
415 tentacular feeding. (*d*–*f*) Simulations of the inhalant current of pharyngeal filter feeding. (*g*–*i*)
416 Simulations of the exhalant current of pharyngeal filter feeding. Red symbols indicate drag
417 force, blue symbols indicate lift force. Triangles indicate results of simulations of the ventral
418 swelling resting on top of the sediment surface, circles indicate results of simulations of the
419 ventral swelling buried in the sediment.
420
421 **Figure 4.** Phylogeny showing feeding modes of extant and extinct deuterostomes (cinctans
422 marked with a †). Blue boxes indicate tentaculate suspension feeding, red boxes indicate
423 pharyngeal filter feeding, green boxes indicate multiple feeding modes.
424
425
426 ## Electronic supplementary material
427
428 **Supplementary Information.** Supplementary methods and figures.
429
430 **Table S1.** Input parameters for the CFD simulations.
431
432 **Table S2.** Drag force and coefficient for the CFD simulations.
433
434 **Table S3.** Lift force and coefficient for the CFD simulations.
435

436 **Table S4.** Drag and lift forces and their coefficients for the sensitivity analyses of mesh size,
437 solver and flow type.
438
439

440 Data available on Dryad

441

442 **Model S1.** Digital reconstruction of *Protocinctus* in VAXML format, compressed in a ZIP
443 archive. To view, unzip the .zip file and open the unpacked .vaxml file with SPIERSview
444 (program and documentation available from www.spiers-software.org).
445

446 **Model S2.** Digitally restored model of *Protocinctus* (operculum in 'closed' position) in IGES
447 format, compressed in a ZIP archive. To view, unzip the .zip file and open the unpacked .igs
448 file with FreeCAD (program and documentation available from www.freecadweb.org).
449

450 **Model S3.** Digitally restored model of *Protocinctus* (operculum in 'open' position) in IGES
451 format, compressed in a ZIP archive. To view, unzip the .zip file and open the unpacked .igs
452 file with FreeCAD (program and documentation available from www.freecadweb.org).
453

454 **Video S1.** Results of a CFD simulation using a time-dependent solver to show flow time-
455 evolution. Simulation of passive tentacular feeding with *Protocinctus* oriented at 180° to the
456 current (ambient velocity of 0.2 m/s) and with the ventral swelling buried within the
457 sediment, visualized as two-dimensional plots (horizontal cross-sections) of flow velocity
458 magnitude (false-colour scale different for each ambient flow velocity) with streamlines over
459 the first 10 s with a time step size of 0.01 s.
460

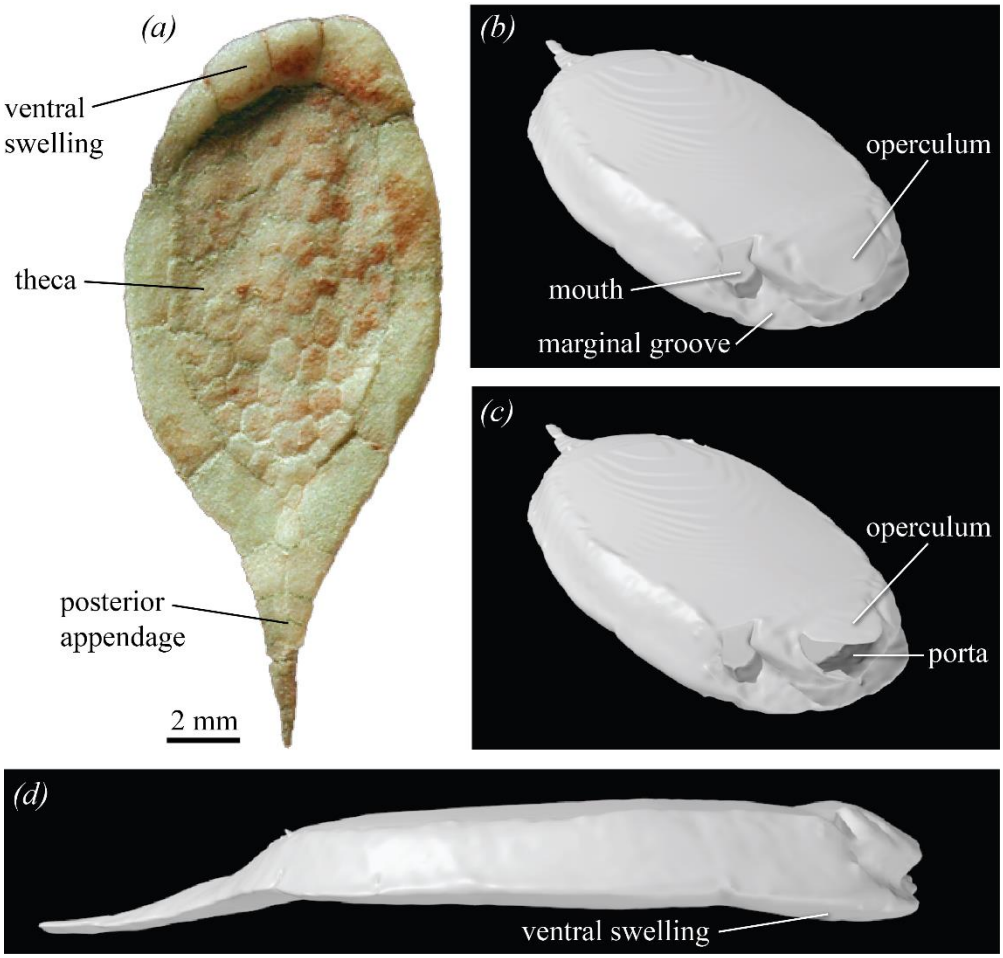
(a)
ventral swelling
theca
posterior appendage
2 mm
(b)
operculum
mouth
marginal groove
(c)
operculum
porta
(d)
ventral swelling

Figure 1.

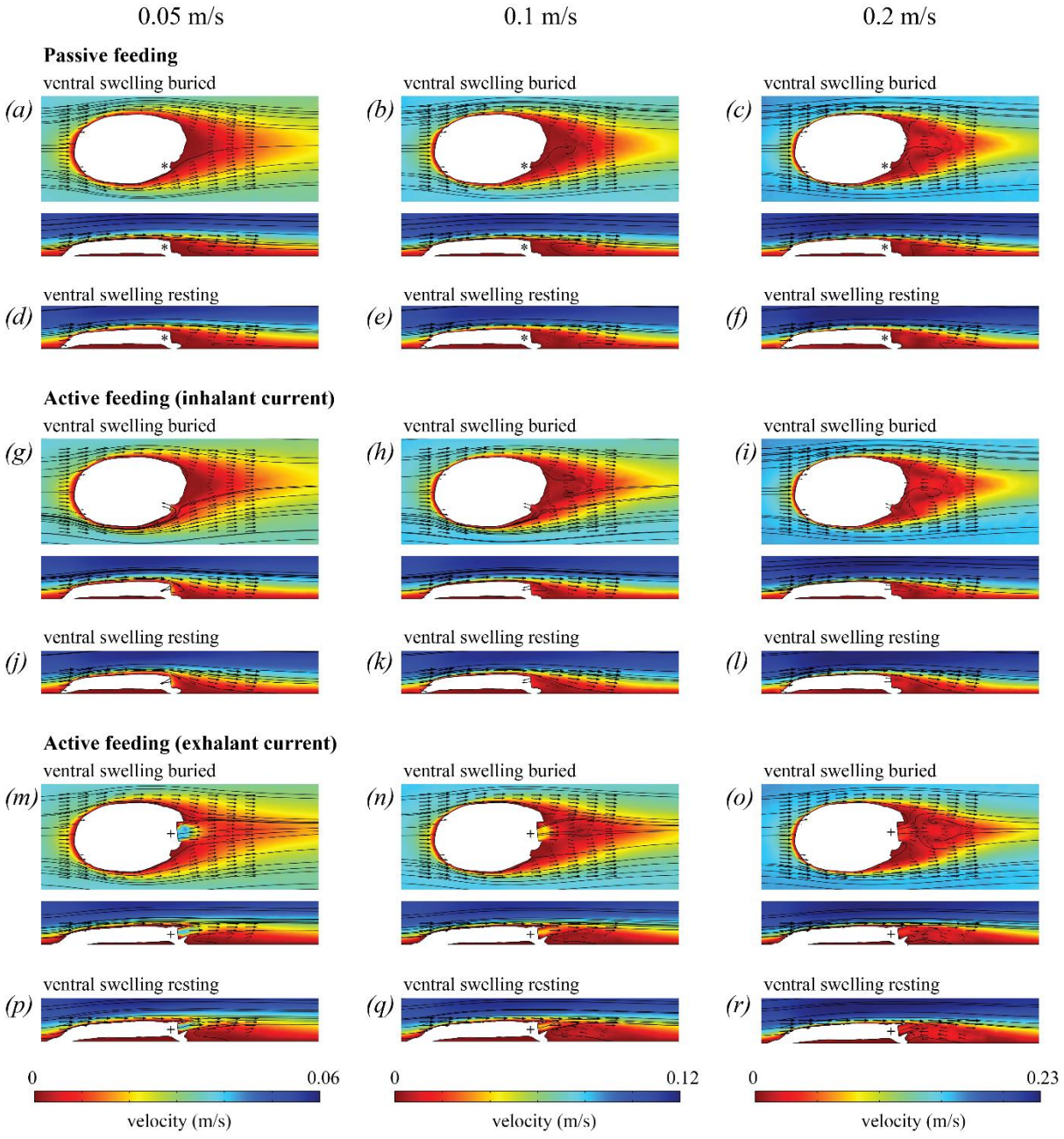

463

464 **Figure 2.**

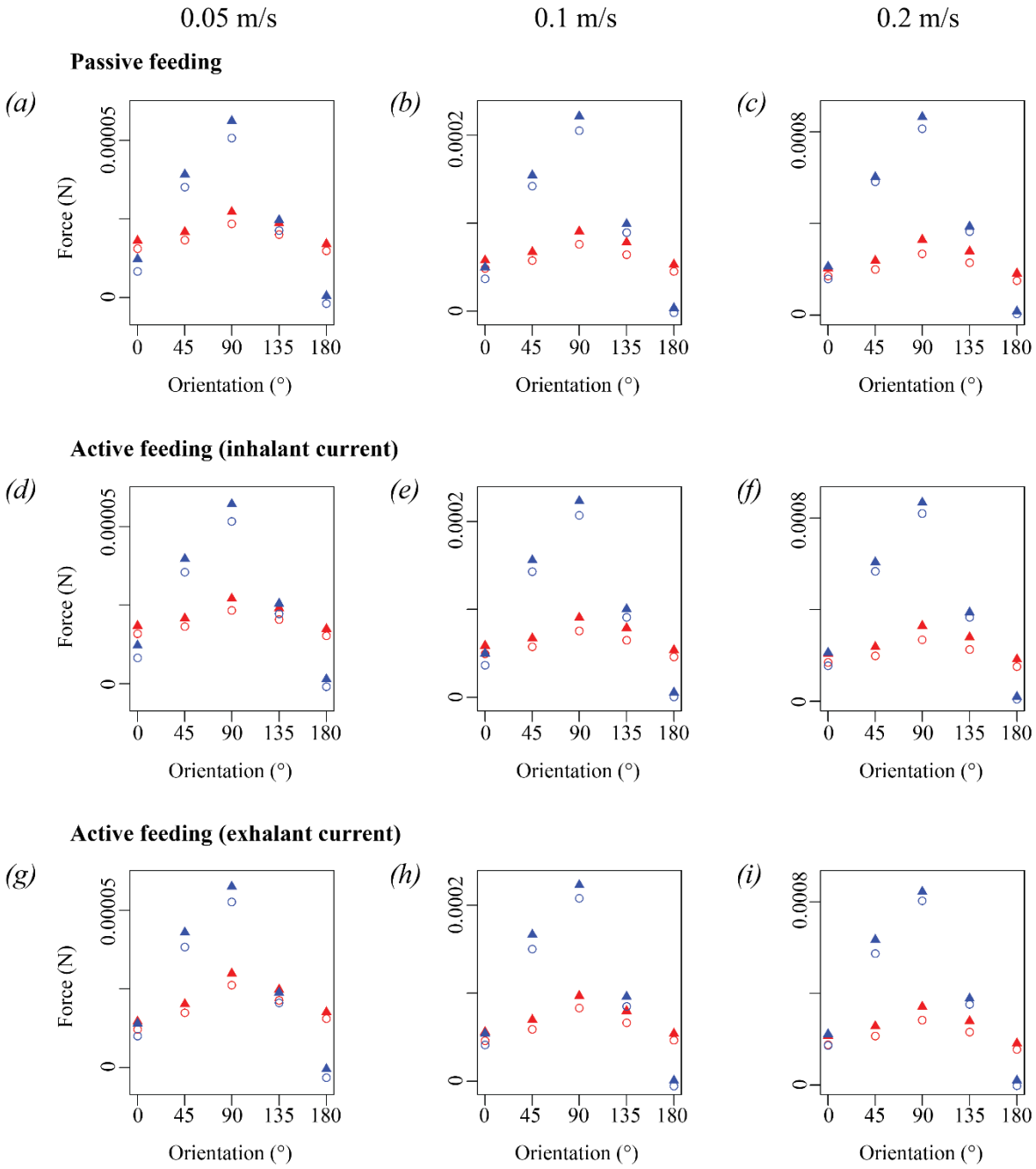

465

466 **Figure 3.**

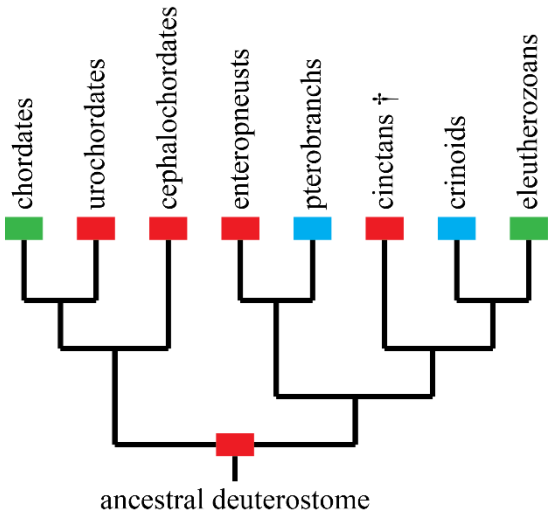

467

468 **Figure 4.**